

AJP

ISSN : 0971 - 3093

Vol 24, No 5, May, 2015

ASIAN JOURNAL OF PHYSICS

An International Quarterly Research Journal



ANITA PUBLICATIONS

FF-43, 1st Floor, Mangal Bazar, Laxmi Nagar, Delhi-110 092, India
B O : 2, Pasha Court, Williamsville, New York-14221-1776, USA



Theoretical investigation of vibrational characteristics and conducting properties of building blocks of organic conductors: TSF, TTF and their cations

Poonam Rani, Omkant Jha and R A Yadav
*Laser and Spectroscopy Laboratory, Department of Physics,
Banaras Hindu University, Varanasi-221 005, India*

Dedicated to Prof J R Durig

Molecular geometries, vibrational spectra along with IR and Raman intensities and depolarization ratios of the Raman lines of the building blocks [Tetrathiafulvalene (TTF), Tetraselenafulvalene (TSF)] of organic conductors along with their cations were investigated at the B3LYP/6-311++G(d,p) level (Gaussian 09 package). The calculated IR and Raman bands have been assigned to different normal modes on the basis of the calculated potential energy distributions (PEDs) and form of the normal mode with the help of Gauss View. Charge transfer occurring in the molecule has been shown by the calculated value of HOMO-LUMO energies. In order to elucidate the transfer of electrons, the vibronic coupling coefficients for the $TSF \rightarrow TSF^+$ and $TTF \rightarrow TTF^+$ transitions have been computed. Involvement of vibrational modes in conduction of molecules has been studied. The vibrational modes $\nu(\text{ring})$ and $\nu(\text{C}=\text{C})$ under the species a_1 contribute considerably to vibronic coupling. Large vibronic coupling constants of these modes show that removal of an electron from TSF and TTF is much easier under the influence of above mentioned vibrational modes. © Anita Publications. All rights reserved.

Keywords: Molecular conductor, DFT, PEDs, HOMO-LUMO, Vibronic coupling, Charge transfer

1 Introduction

The past few years have seen a large number of theoretical investigations in the field of organic conductors [1,2]. Common features that control the performance of the devices based on organic conductors are molecular structure, electronic structure, electronic properties, charge transport properties, charge injection or collection, charge transport across the active layers [3-6], charge recombination or separation [7,8], dynamics of exciton formation or dissociation [9-11], energy transfer in the bulk material [12-14], supramolecular organization of the samples [15], inter chain interactions [16,17], chemical and structural defects [18] and absorption or emission properties [19,20]. Despite the interesting major advances made recently, additional work needs to be done concerning the computational methods actually in use because of comprehensive understanding at the microscopic level of all the phenomena involving the application of higher and higher levels of theory over a larger set of materials [21].

{[2,2]-Bi([1,3]diselenolylidene)}≡tetraselenafulvalene (TSF) and {[2-(1,3-dithiole-2-ylidene)-1,3-dithiole]≡tetrathiafulvalene (TTF)} are the core building blocks of the conducting organic materials. These types of materials have received much attention as they show a wide ranged electrical conductivity (from insulators and semiconductors to metals and superconductors). Owing to strong coupling between geometrical and electronic structures [22-24] localized charge carriers remain on individual molecules for enough time to allow relaxation of the nuclei in order to accommodate the new state. In the next step, which is normally driven by an externally applied electric field, the charge carriers jump along sufficiently ordered crystal structures from one molecule to the closest one; the latter being initially in the neutral state and the former in the ionized state. This mechanism is widely known as the hopping regime [25]. The rate of transfer of the charge carriers critically depends on the reorganization energy and vibronic coupling.

Corresponding author :

e-mail: rayadav@bhu.ac.in; ray1357@gmail.com; Tel.: +91 542 2368593; fax: +91 542 2368390 (R A Yadav)

Some theoretical calculations of the fundamental frequencies of TSF have been done to compare the absorption of the Ag on the surface of TSF [26]. However, to the best of our knowledge the complete IR and Raman frequencies of the TSF and its cation molecules have not been carried out yet. Therefore in the present study, we have planned to investigate the Raman and IR spectra along with the measurement of depolarization ratios of the Raman lines for TSF and its cation. To make the study more complete, we have included the data on TTF and its cation from our earlier study [27]. The vibrational mode assignments for the observed wavenumbers have been made in the light of the potential energy distributions (PEDs). It is also planned to study the charge transport phenomena in the TSF and TTF molecules in order to understand their conducting behavior, for which detailed analysis of their electron-molecular-vibration coupling constant, relaxation energy for each totally symmetric mode have been carried out. The present investigation also includes the study of electronic and electrical properties of TSF and TTF along with their corresponding radical cations.

2 Computational details

The optimized molecular geometries, APT charges and fundamental vibrational wavenumbers along with their corresponding intensities in IR spectrum, Raman activities and depolarization ratios of the Raman bands for TSF, TTF and with their corresponding cations have been computed at the B3LYP/6-311++G** level using Gaussian 09 [28] program package. For the cation radicals the optimized geometries of the neutral molecules were taken as the input structures and calculations were performed. The geometries were fully optimized by minimizing the energies with respect to all the geometrical parameters without imposing any molecular symmetry constraints. The assignments of the normal modes were made by visual inspection of the individual mode using the Gauss View software [29]. The optimized geometries and frontier MOs were viewed with the help of this software.

For the normal coordinate analysis (NCA), the force field obtained in the Cartesian coordinates and the dipole derivatives with respect to the atomic displacements were extracted from the archive section of the Gaussian 09 output file and transformed to a suitably defined set of internal coordinates by means of GAR2PED software [30]. For the study of vibronic coupling, the calculations were performed with the B3LYP/6-311++G** method to obtain the normal modes u_A^i and the gradient of the total electronic energy $\left(\frac{\partial E(r,R)}{\partial R_i}\right)_{R_0}$. Vibronic coupling constants (VCCs) of the TSF \rightarrow TSF⁺ and TTF \rightarrow TTF⁺ transitions were investigated and analyzed.

3 Result and Discussions

3.1 Geometrical Structures

Figure 1 presents the labeling scheme of TSF. The optimized geometrical parameters of TSF, TTF and their cations are collected in Table 1 and their structures are shown in Fig 2. The present calculations predicted that the TSF and TTF molecules have non-planar structure with C_{2v} point symmetry while their corresponding cations have planar structures with D_{2h} point symmetry. The C₂ axis is taken as the z-axis for all the molecules. In neutral molecules, the atoms C₁, C₁₀, Se/S₁₁, Se/S₁₂, Se/S₁₃ and Se/S₁₄ are co-planar (xy plane). The C₂(z) axis passes through the center of the C₁=C₁₀ bond and the XZ and YZ are the symmetry planes for the neutral molecules.

The optimised bond length for C₁=C₁₀ for TSF and as well for TTF is larger than the usual C=C bond length (1.33 Å) while the bond lengths C₂=C₃ and C₇=C₈ are approximately in the range of the C=C bond length. Due to the removal of an electron from the neutral molecules the bond length C₁=C₁₀ is enhanced by

0.05 Å and the bond lengths $C_2=C_3$, $C_7=C_8$ are enhanced by 0.008 Å. The optimized bond lengths of C_1-Se/S_{11} , C_1-Se/S_{12} , $C_{10}-Se/S_{13}$ and $C_{10}-C_{14}$ are larger than C_2-Se/S_{11} , C_3-Se/S_{12} , C_7-Se/S_{13} and C_8-Se/S_{14} for TSF as similar to TTF [27]. The latter bond lengths are shortened by ~ 0.13 Å, whereas the former bond lengths are shortened by 0.024 Å in going from neutral molecules to their corresponding cations. The lengthening of all the central bonds (C_1-C_{10} , C_1-Se/S_{11} , C_1-Se/S_{12} , $C_{10}-Se/S_{13}$ and $C_{10}-Se/S_{14}$) as compared to the edge bonds (C_2-C_3 , C_7-C_8 , C_2-Se/S_{11} , C_3-Se/S_{12} , C_7-Se/S_{13} and C_8-Se/S_{14}) could be due to the strong antibonding character between the S atoms of two different rings. As the energy of the antibonding orbitals are always negative, the atoms of the molecule are repelled and bond lengths are increased [27]. The TSF, TSF^+ , TTF and TTF^+ molecules exhibit partial double bond character. The partial double bond character has been found to be indicative of the conducting behavior of TSF and its cation as similar to TTF [27]. No major changes are noticed for the C-H bond lengths.

Table 1. Computed geometrical parameters* of TSF, TTF and their cations.

Definition	TSF	TSF^+	TTF	TTF^+
$r(C_1=C_{10})$	1.343	1.388	1.347	1.396
$r(C_1-S/Se_{11})$	1.929	1.894	1.785	1.746
$r(C_1-S/Se_{12})$	1.929	1.894	1.785	1.746
$r(C_2=C_3)$	1.332	1.3389	1.334	1.343
$r(C_2-H_4)$	1.083	1.083	1.081	1.082
$r(C_2-Se/S_{11})$	1.905	1.8805	1.762	1.74
$r(C_3-H_5)$	1.083	1.083	1.081	1.082
$r(C_3-Se/S_{12})$	1.905	1.8805	1.762	1.74
$r(H_6-C_7)$	1.083	1.083	1.081	1.082
$r(C_7=C_8)$	1.332	1.3389	1.334	1.343
$r(C_7-Se/S_{13})$	1.905	1.8805	1.762	1.74
$r(C_8-H_6)$	1.083	1.083	1.081	1.082
$r(C_8-Se/Se/S_{14})$	1.905	1.8805	1.762	1.740
$r(C_{10}-Se/S_{13})$	1.929	1.894	1.785	1.745
$r(C_{10}-Se/Se/S_{14})$	1.929	1.894	1.785	1.745
$\alpha(C_{10}-C_1-Se/S_{11})$	123.463	123.0003	123.221	122.802
$\alpha(C_{10}-C_1-Se/S_{12})$	123.463	123.0003	123.22	122.802
$\alpha(Se/S_{11}-C_1-Se/S_{12})$	113.074	113.9994	113.558	114.395
$\alpha(C_3-C_2-H_4)$	124.021	124.3068	124.956	125.444
$\alpha(C_3-C_2-Se/S_{11})$	119.686	119.257	117.971	117.222
$\alpha(H_4-C_2-Se/S_{11})$	116.280	116.4363	117.055	117.333
$\alpha(C_2-C_3-H_5)$	124.021	124.3068	124.956	125.444
$\alpha(C_2-C_3-Se/S_{12})$	119.686	119.2569	117.971	117.222
$\alpha(H_5-C_3-Se/S_{12})$	116.280	116.4362	117.054	117.334
$\alpha(H_6-C_7-C_8)$	124.021	124.3068	124.956	125.444
$\alpha(H_6-C_7-Se/S_{13})$	116.280	116.4362	117.054	117.334
$\alpha(C_8-C_7-Se/S_{13})$	119.686	119.257	117.971	117.222

α (C ₇ -C ₈ -H ₉)	124.021	124.3068	124.956	125.444
α (C ₇ -C ₈ -Se/S ₁₄)	119.686	119.257	117.971	117.222
α (H ₉ -C ₈ -Se/S ₁₄)	116.280	116.4362	117.054	117.334
α (C ₁ -C ₁₀ -Se/S ₁₃)	123.463	123.0003	123.220	122.802
α (C ₁ -C ₁₀ -Se/S ₁₄)	123.463	123.0003	123.220	122.802
α (S/Se ₁₃ -C ₁₀ -Se/S ₁₄)	113.074	113.9994	113.558	114.395
α (C ₁ -Se/S ₁₁ -C ₂)	92.744	93.7433	94.665	95.8
α (C ₁ -Se/S ₁₂ -C ₃)	92.744	93.7433	94.665	95.8
α (C ₇ -Se/S ₁₃ -C ₁₀)	92.744	93.7433	94.665	95.58
α (C ₈ -Se/S ₁₄ -C ₁₀)	92.744	93.7433	94.665	95.58
δ (Se/S ₁₁ -C ₁ -C ₁₀ -Se/S ₁₃)	-0	0.004	179.707	0.003
δ (Se/S ₁₁ -C ₁ -C ₁₀ -Se/S ₁₄)	179.635	179.999	0.001	-179.967
δ (Se/S ₁₂ -C ₁ -C ₁₀ -Se/S ₁₃)	-179.636	180.01	0.001	179.975
δ (Se/S ₁₂ -C ₁ -C ₁₀ -Se/S ₁₄)	0	0.004	-179.705	0.004
δ (C ₁₀ -C ₁ -Se/S ₁₁ -C ₂)	166.666	-180.01	169.853	-180.02
δ (S ₁₂ -C ₁ -Se/S ₁₁ -C ₂)	-13.664	-0.015	-10.416	0.007
δ (C ₁₀ -C ₁ -Se/S ₁₂ -C ₃)	-166.666	180.01	-169.854	180.019
δ (Se/S ₁₁ -C ₁ -Se/S ₁₂ -C ₃)	13.664	0.016	10.414	-0.006
δ (H ₄ -C ₂ -C ₃ -H ₅)	0.0	0	0.001	0
δ (H ₄ -C ₂ -C ₃ -Se/S ₁₂)	178.637	180.01	178.377	179.995
δ (Se/S ₁₁ -C ₂ -C ₃ -H ₅)	-178.637	-180.01	-178.38	-179.994
δ (Se/S ₁₁ -C ₂ -C ₃ -Se/S ₁₂)	0.0	0.001	-0.004	0.001
δ (C ₃ -C ₂ -Se/S ₁₁ -C ₁)	-8.623	-0.010	-6.436	-0.005
δ (H ₄ -C ₂ -Se/S ₁₁ -C ₁)	172.637	-180.019	175.054	180.001
δ (C ₂ -C ₃ -Se/S ₁₂ -C ₁)	8.623	0.0092	6.441	0.003
δ (H ₅ -C ₃ -Se/S ₁₂ -C ₁)	-172.637	180.018	-175.053	-180.001
δ (H ₆ -C ₇ -C ₈ -H ₉)	0.0	0	0.001	0
δ (H ₆ -C ₇ -C ₈ -Se/S ₁₄)	-178.637	-180.01	-178.38	180.006
δ (Se/S ₁₃ -C ₇ -C ₈ -H ₉)	178.637	180.01	178.377	-180.006
δ (Se/S ₁₃ -C ₇ -C ₈ -Se/S ₁₄)	0.0	0.001	-0.003	0.001
δ (H ₆ -C ₇ -Se/S ₁₃ -C ₁₀)	-172.637	180.018	-175.053	-179.991
δ (C ₈ -C ₇ -Se/S ₁₃ -C ₁₀)	8.623	0.009	6.441	0.013
δ (C ₇ -C ₈ -Se/S ₁₄ -C ₁₀)	-8.623	-0.01	-6.437	-0.014
δ (H ₉ -C ₈ -Se/S ₁₄ -C ₁₀)	172.637	-180.019	175.054	179.991
δ (C ₁ -C ₁₀ -Se/S ₁₃ -C ₇)	-166.666	180.01	169.853	-179.995
δ (Se/S ₁₄ -C ₁₀ -Se/S ₁₃ -C ₇)	13.664	0.016	-10.416	-0.023
δ (C ₁ -C ₁₀ -Se/S ₁₄ -C ₈)	166.666	-180.01	-169.854	179.996
δ (Se/S ₁₃ -C ₁₀ -Se/S ₁₄ -C ₈)	-13.664	-0.016	10.415	0.023

* : Bond lengths (r) in Å, bond angles (α) and dihedral angles (δ) in degrees ($^\circ$).

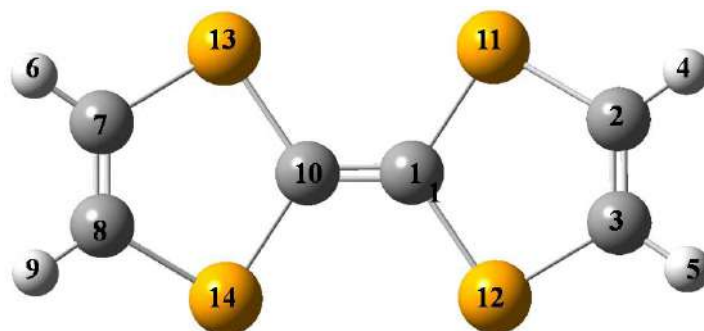


Fig 1. Labelling structure of TTF

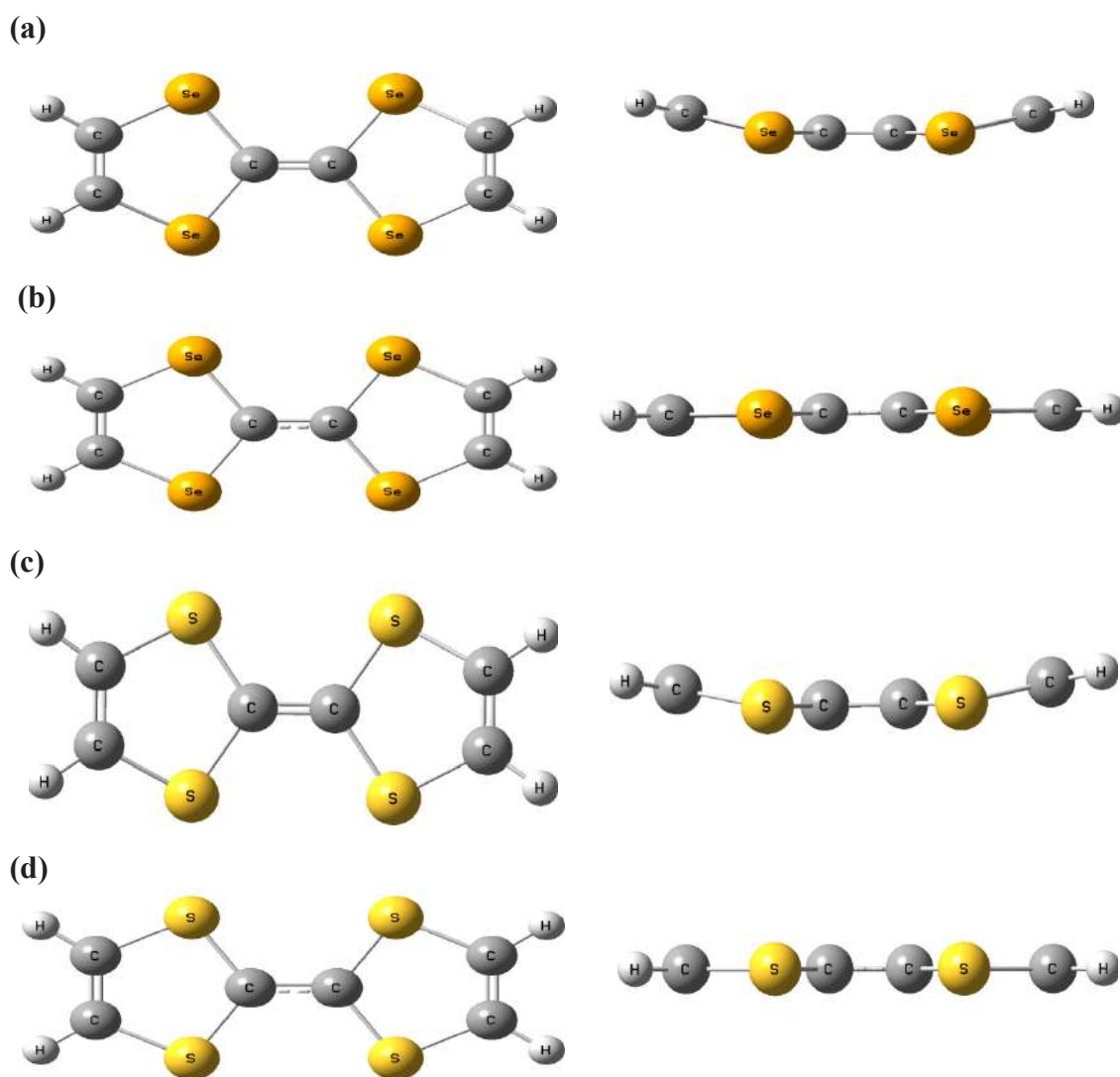


Fig 2. Front and side views of (a) TTF (b) TTF⁺ (c) TTF (d) TTF⁺

The bond angles $\alpha(\text{C}_{10}\text{-C}_1\text{-Se/S}_{11})$, $\alpha(\text{C}_{10}\text{-C}_1\text{-Se/S}_{12})$, $\alpha(\text{C}_1\text{-C}_{10}\text{-Se/S}_{13})$ and $\alpha(\text{C}_1\text{-C}_{10}\text{-Se/S}_{14})$ are same for TSF and TTF and are decreased by 0.5° in going from neutral to their corresponding cations. It is to be noticed that the bond angles $\alpha(\text{C}_3\text{-C}_2\text{-Se/S}_{11})$, $\alpha(\text{C}_2\text{-C}_3\text{-Se/S}_{12})$, $\alpha(\text{C}_6\text{-C}_7\text{-Se/S}_{13})$ and $\alpha(\text{C}_8\text{-C}_7\text{-Se/S}_{14})$ in TSF is decreased by $\sim 2^\circ$ as compared to TTF, whereas in going from the neutral molecules to their corresponding cations these angles are decreased by $\sim 0.5^\circ$. The bond angles $\alpha(\text{Se/S}_{11}\text{-C}_1\text{-Se/S}_{12})$ and $\alpha(\text{Se/S}_{13}\text{-C}_{10}\text{-Se/S}_{14})$ in TSF are smaller than those in TTF by $\sim 0.5^\circ$ and in going from neutral to their corresponding cations these bond angles are increased by $\sim 1^\circ$.

The dihedral angles of the optimised structures for TSF and TTF molecules are also included in [Table 1](#).

3.2 Atomic charges

The sum of charge tensor and charge flux tensor is referred to as atomic polarizability tensor (APT) [31]. APT atomic charges (in unit of e) at each atomic site of TSF, TTF and their cations are collected in [Table 2](#). It is noted from the [Table 2](#) that all the Se atoms of TSF possess positive charge having negligible small magnitudes, whereas all the S atoms of TTF possess negative charge having magnitude 0.36 e. In going from TSF/TTF to $\text{TSF}^+/\text{TTF}^+$, the positive atomic charges at all the Se/S sites gain positive charge by 0.21/0.14, indicating that the Se/S atoms of TSF/TTF have ability to donate charge. All the C atoms of the TSF molecule possess negative charges. The magnitudes of the central C atoms are 0.26e and of the edge C atoms are 0.16e. On the other hand in the TTF molecule, two central C atoms possess positive charges of magnitude in 0.49e and the remaining four C atoms of the pentagon rings possess negative charges of magnitude 0.1e.

Table 2. Calculated APT charges* at various atomic sites of TSF, TTF and their cations.

Symbol	TSF	TSF ⁺	TTF	TTF ⁺
C ₁	-0.26	-0.232	0.49	0.51
C ₂	-0.16	-0.173	-0.10	-0.07
C ₃	-0.16	-0.173	-0.10	-0.07
H ₄	0.24	0.285	0.22	-0.29
H ₅	0.24	0.285	0.22	-0.29
H ₆	0.24	0.285	0.22	-0.29
C ₇	-0.16	-0.173	-0.10	-0.07
C ₈	-0.16	-0.173	-0.10	-0.07
H ₉	0.24	0.285	0.22	-0.29
C ₁₀	-0.26	-0.232	0.49	0.51
Se ₁₁ /S ₁₁	0.05	0.254	-0.36	-0.22
Se ₁₂ /S ₁₂	0.05	0.254	-0.36	-0.22
Se ₁₃ /S ₁₃	0.05	0.254	-0.36	-0.22
Se ₁₄ /S ₁₄	0.05	0.254	-0.36	-0.22

*: Charges in e

A perusal of [Table 2](#), suggests that in going from TSF to TSF^+ the magnitude of the charges of C₁, and C₁₀ atoms decrease, while the magnitude of the all other C, H and Se atoms increase. In going from TTF to TTF^+ the magnitude of the charges of the C₁, C₁₀ and all H atoms increase, whereas the magnitude of the charges of the remaining four C and four S atoms decrease.

3.3 Electronic structure and properties

The higher value of the energy of HOMO level (E_{HOMO}) of a molecule means it has good tendency to donate an electron while the lower value of the energy of LUMO level (E_{LUMO}) of a molecule means it has good tendency to accept an electron. Knowledge of energies of the HOMO and LUMO is essential to govern many chemical reactions and determining electronic band gaps in solids [32-34]. The energy of the E_{HOMO} of TSF and TTF molecules is calculated to be -4.3eV and -4.8eV i.e. $\sim -5\text{eV}$, whereas the energy of the LUMO of TSF is -1.0eV and that of TTF is -1.1eV , as a consequence the TSF molecule has higher tendency to donate the electrons as compared to the TTF molecule.

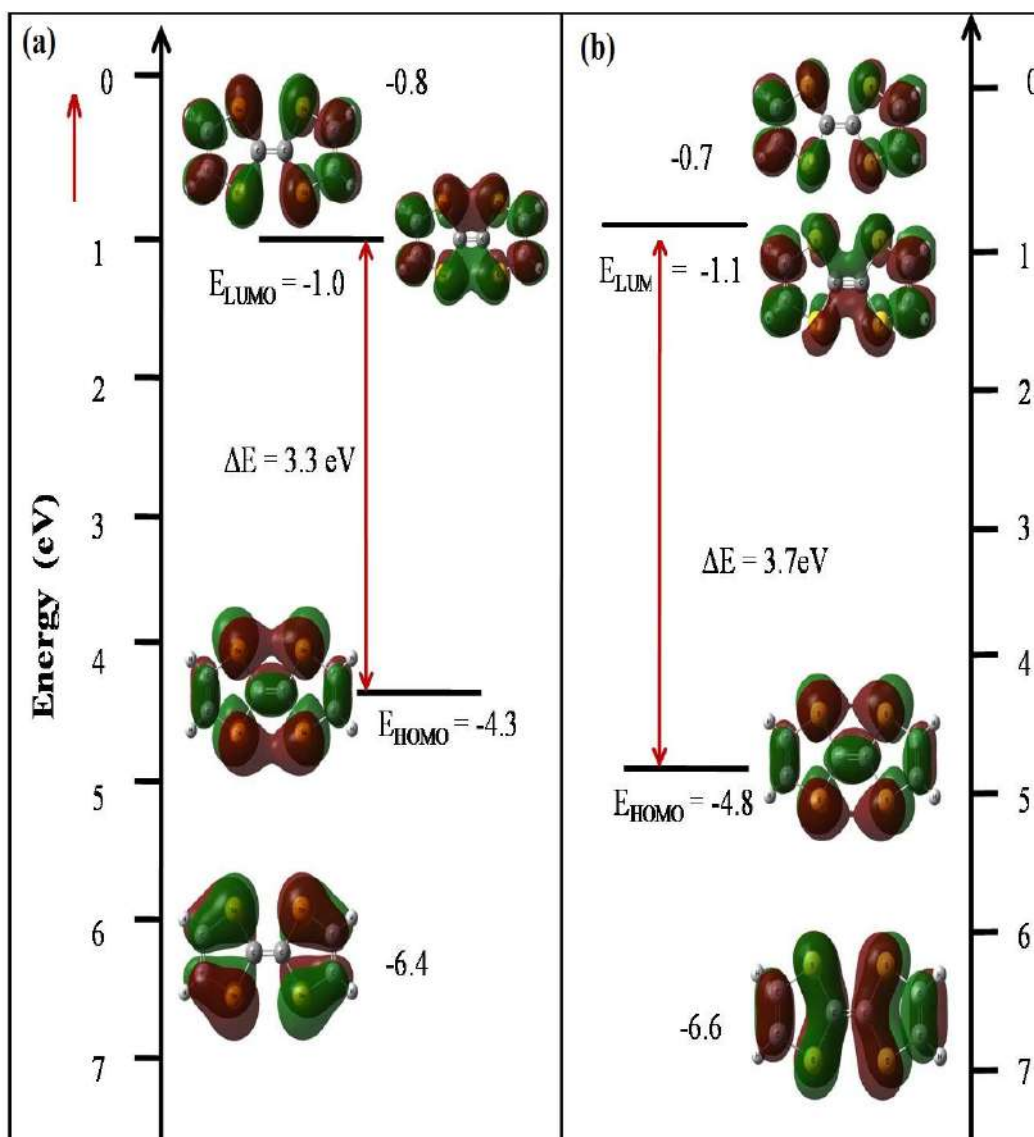


Fig 3. Energy level diagram of the frontier MOs for (a) TSF and (b) TTF

The energy gap, $\Delta E = E_{\text{LUMO}} - E_{\text{HOMO}}$, is a quantitative measure of the kinetic stability of the molecule [35, 36]. A large value of the energy gap implies high kinetic stability and low chemical reactivity because it is energetically unfavorable to add electrons to a high lying LUMO to remove electrons from a low lying HOMO and activate to complex formation of any potential reaction [37]. The present calculations show that the energy gap of the TTF molecule is greater than that the TSF molecule by 0.44 eV, Fig 3 and therefore, the TTF molecule is found to be kinetically more stable and chemically less reactive as compared to the TSF molecule.

A molecule with high ionization potential (IP) means that it does not lose electron easily [38, 39]. A molecule with greater electron affinity (EA) tends to accept an electron easily [38, 39]. Employing Koopmans' approximation [40], the ionization potential and electron affinity can be calculated using the relations,

$$\text{IP} = -E_{\text{HOMO}} \quad (3)$$

$$\text{EA} = -E_{\text{LUMO}} \quad (4)$$

It has been discussed earlier that both the neutral molecules have the same tendency to lose electrons and hence, have the same ionization potential but TSF molecule would take electrons more easily as compared to the TTF molecule. Therefore, TTF molecule has greater electron affinity.

3.4 Vibrational Assignments

The 36 normal modes of vibration of all the studied molecules are given in Table 3. The harmonic-vibrational frequencies calculated for TSF, TTF and their cations using the B3LYP/6-311++G** method have been collected in the Table 3. The *ab initio* methods provide the vibrational frequencies which are overestimated due to neglect of anharmonicity in the real systems. The computed IR and Raman spectra for the four examined molecules are shown in Fig 4 and Fig 5, respectively.

Table 3. Calculated and experimental wavenumbers (cm^{-1}) of TSF, TTF and their cations.

Sr no.	TSF	TSF ⁺	TTF		TTF ⁺	Species	PEDs
			Calculated	Experimental IR Raman			
1.	46	23	80		42	a ₂	$\tau(\text{C}_1\text{-C}_{10})(92)$
	(0,0.03)	(0,0)	(0,0.04)	-	(0,0)		
	0.75	0.68	0.75		0.65		
2.	47	71	39		83	a ₁	$\Phi(\text{ring})(42)\text{-}\Phi(\text{ring})(42)$
	(2.15,0.45)	(3.96,0)	(3.80,0.51)	-	(4.44,0)		
	0.28	0.07	0.16		0.74		
3.	60	94	80	105	143	b ₂	$\Phi(\text{ring})(45)\text{+}\Phi(\text{ring})(45)$
	(1.059,1.50)	(0,2.69)	(0.19,0.19)	(w)	(0,0.46)		
	0.75	0.75	0.75		0.75		
4.	76	81	109	114	117	b ₁	$\beta(\text{C}_1\text{=C}_{10})(49)\text{-}\beta(\text{C}_1\text{=C}_{10})(49)$
	(0.14,0.022)	(0.040,0)	(0.59,0.07)	(w)	(0.28,0)		
	0.75	0.62	0.75		0.75		

5	154	167	237	-	-	264	a ₁	$\gamma(C_1=C_{10})(22)+$
	(0.083,6.70)	(0,18.14)	(0.17,12.60)			(0,29.16)		$\gamma(C_1=C_{10})(22)-\alpha(\text{ring})$ (15)- $\alpha(\text{ring})$ (
	0.25	0.27	0.26			0.28		
6	185	180	306	-	308 (m)	300	a ₂	$\beta(C_1=C_{10})(25)+\beta(C_1=C_{10})$ (25)+ $v(C_{10}-S_{11})(11)+$ $v(C_1-S_{13})(11)-v(C_{10}-S_{12})$ (11)- $v(C_1-S_{14})(11)$
	(0,4.38)	(0,1.67)	(0,8.96)			(0,3.92)		
	0.75	0.75	0.75			0.75		
7	222	267	267	255	-	326	a ₁	$\gamma(C_1=C_{10})(21)+$
	(1.99,1.41)	(3.74,0)	(0.69,3.84)			(2.20,0.01)		$\gamma(C_1=C_{10})(21)+ \alpha(\text{ring})$ (13)+ $\alpha(\text{ring})(13)$
	0.53	0.11	0.30	(w)		0.24		
8	253	273	430	434	-	469	b ₂	$\alpha(\text{ring})(33)-\alpha(\text{ring})(33)$
	(3.27,0.004)	(3.50,0)	(14.95,0.05)			(15.37,0)		
	0.75	0.69	0.75	(w)		0.72		
9	280	289	471	-	474	505	a ₁	$v(C_1-S_{14})(16)+ v(C_1-$ $S_{13})(16)+v(C_{10}-S_{12})$ (16)+ $v(C_{10}-S_{11})$ (16)+ $\alpha(\text{ring})(16)+\alpha(\text{ring})$ (16)
	(0.55,8.12)	(0,54.33)	(0.02,14.59)			(0,87.88)		
	0.44	0.119	0.65	(m)		0.13		
10	381	380	411	-	420 (w)	411	a ₂	$\Phi(\text{ring})(40)+\Phi(\text{ring})(40)$
	(0,0.005)	(0,0)	(0,0.28)			(0,0)		
	0.75	0.72	0.75			0.61		
11	388	392	416	412	-	428	b ₁	$\Phi(\text{ring})(40)-\Phi(\text{ring})(40)$
	(0.081,4.2)	(0,2.68)	(0,3.16)			(0,1.8)		
	0.75	0.75	0.75	(vw)		0.75		
12	472	480	515	-	-	521	b ₂	$\gamma(C_1=C_{10})(44)-\gamma(C_1=C_{10})$ (44)
	(0,0.024)	(0,0.09)	(2.74,0.52)			(0,0.15)		
	0.75	0.75	0.75			0.75		
13	483	496	613	-	612	629	a ₂	$\alpha(\text{ring})(23)-\alpha(\text{ring})(23)-$ $v(C_3-S_{13})(12)+ v(C_2-S_{14})$ (12)- $v(C_7-S_{11})(12)+v(C_8-$ $S_{12})(12)$
	(0,0.27)	(0,17.75)	(0,0.19)			(0,11.44)		
	0.75	0.75	0.75	(vw)		0.75		
14	487	501	623	619	-	639	b ₁	$\alpha(\text{ring})(23)+\alpha(\text{ring})$ (23)+ $v(C_7-S_{11})(13)-v(C_8-$ $S_{12})(13)-v(C_3-S_{13})(13)+$ $v(C_2-S_{14})(13)$
	(0.47,0.070)	(0.95,0)	(1.93,0.04)			(0.90,0)		
	0.75	0.51	0.75	(vw)		0.74		

	572	895	864		885		$\gamma(\text{C}_2\text{-H}_4)(23)-\gamma(\text{C}_3\text{-H}_5)$
15	(0.30,0.103)	(0,0.16)	(0.18,0.48)	864	-	(0,0.0038)	$(23)+\gamma(\text{C}_8\text{H}_9)(23)-\gamma(\text{C}_7\text{-H}_6)(23)-\Phi(\text{ring})(4)-\Phi(\text{ring})(4)$
	0.75	0.75	0.75	(vw)		0.75	
	581	596	726		735		$\nu(\text{C}_3\text{-S}_{13})(23)+\nu(\text{C}_2\text{-S}_{14})$
16	(2.43,1.155)	(2.0,0)	(10.41,0.19)	732	-	(7.48,0)	$(23)-\nu(\text{C}_7\text{-S}_{11})(23)-\nu(\text{C}_8\text{-S}_{12})(23)$
	0.75	0.63	0.75	(m)		0.74	
	595	614	729		735	746	$\nu(\text{C}_7\text{-S}_{11})(24)+\nu(\text{C}_8\text{-S}_{12})$
17	(5.64,39.96)	(0,11.28)	(0.01,18.59)	-	(m)	(0,8.80)	$(24)+\nu(\text{C}_3\text{-S}_{13})(24)+\nu(\text{C}_2\text{-S}_{14})(24)$
	0.20	0.08	0.14		0.11	0.41	
	620	673	643			696	$\gamma(\text{C}_7\text{-H}_6)(25)+\gamma(\text{C}_8\text{H}_9)$
18	(8.75,3.47)	(0.0001,1.28)	(2.14,2.89)	655 sh	-	(0,0.73)	$(25)-\gamma(\text{C}_3\text{-H}_5)(25)-\gamma(\text{C}_2\text{-H}_4)(25)$
	0.75	0.75	0.75			0.75	
	624	676	644		645	700	$\gamma(\text{C}_3\text{-H}_5)(25)+\gamma(\text{C}_2\text{-H}_4)$
19	(116,12.39)	(130.15,0)	(130,2.34)	645	-	(134.68,0)	$(25)+\gamma(\text{C}_7\text{-H}_6)(25)+\gamma(\text{C}_8\text{H}_9)(25)$
	0.28	0.61	0.29	(vs)		0.49	
	672	702	772		778	819	$\alpha(\text{ring})(17)-\alpha(\text{ring})(17)+\nu(\text{C}_1\text{-S}_{14})(16)-\nu(\text{C}_{10}\text{-S}_{12})$
20	(7.07,0.57)	(32.56,0)	(25.88,0.20)	778	-	(39.03,0)	$(16)+\nu(\text{C}_1\text{-S}_{13})(16)-\nu(\text{C}_{10}\text{-S}_{11})(16)$
	0.75	0.74	0.75	(s)		0.75	
	708	759	827		796	879	$\nu(\text{C}_{10}\text{-S}_{11})(18)-\nu(\text{C}_1\text{-S}_{13})$
21	(0.16,0.45)	(19.67,0)	(3.14,0.20)	796	-	(7.11,0)	$(18)-\nu(\text{C}_{10}\text{-S}_{12})(18)+\nu(\text{C}_1\text{-S}_{14})(18)+\alpha(\text{ring})$
	0.75	0.18	0.75	(sh)		0.74	$(11)+\alpha(\text{ring})(11)$
	724	746	799		800	828	$\alpha(\text{ring})(25)-\alpha(\text{ring})$
22	(0,14.30)	(0,18.08)	(0,22.44)	-	(m)	(0,14.03)	$(25)+\nu(\text{C}_8\text{-S}_{12})(12)-\nu(\text{C}_7\text{-S}_{11})(12)+\nu(\text{C}_2\text{-S}_{14})(12)-\nu(\text{C}_3\text{-S}_{13})(12)$
	0.75	0.75	0.75		0.77	0.75	
	725	740	793		794	828	$\alpha(\text{ring})(17)+\alpha(\text{ring})(17)+\nu(\text{C}_3\text{-S}_{13})(11)-\nu(\text{C}_2\text{-S}_{14})$
23	(42.97,0.37)	(3.32,0)	(54.87,0.15)	794	-	(24.70,0)	$(11)-\nu(\text{C}_7\text{-S}_{11})(11)+\nu(\text{C}_8\text{-S}_{12})(11)$
	0.75	0.748	0.75	(vs)		0.75	
	872	893	864		852	882	$\gamma(\text{C}_8\text{H}_9)(23)-\gamma(\text{C}_7\text{-H}_6)$
24	(0,0.044)	(0,0)	(0,0.02)	852	-	(0,0)	$(23)-\gamma(\text{C}_2\text{-H}_4)(23)+\gamma(\text{C}_3\text{-H}_5)(23)-\Phi(\text{ring})$
	0.75	0.73	0.75	(vw)		0.33	$(4)+\Phi(\text{ring})(4)$
	879	932	969		994	1028	$\beta(\text{C}_1=\text{C}_{10})(22)+\beta(\text{C}_1=\text{C}_{10})$
25	(0,0.40)	(0,1.9)	(0,4.16)	-	(vw)	(0,0.0374)	$(22)-\nu(\text{C}_1\text{-S}_{13})(13)+\nu(\text{C}_1\text{-S}_{14})(13)-\nu(\text{C}_{10}\text{-S}_{11})(13)+\nu(\text{C}_{10}\text{-S}_{12})(13)$
	0.75	0.75	0.75		0.77	0.75	
	1105	1118	1120		1088	1128	$\beta(\text{C}_3\text{-H}_5)(24)-\beta(\text{C}_2\text{-H}_4)$
26	(0.0043,0.35)	(0,12.68)	(2.10,0.015)	1088	-	(0.016,0)	$(24)-\beta(\text{C}_7\text{-H}_6)(24)+\beta(\text{C}_8\text{-H}_9)(24)$
	0.75	0.11	0.75	(w)		0.13	

27	1105 (0.18,20.83) 0.47	1119 (0.21,0) 0.17	1121 (0.33,24.04) 0.52	1097 (w)	-	1128 (0,18.44) 0.10	a ₁	$\beta(\text{C}_7\text{-H}_6)(24)-\beta(\text{C}_8\text{-H}_9)(24)+\beta(\text{C}_3\text{-H}_5)(23)-\beta(\text{C}_2\text{-H}_4)(23)$
28	1259 (0,2.40) 0.75	1270 (5.11,0.001) 0.75	1283 (0,0.02) 0.75	1253 (m)	-	1291 (0.68,0) 0.75	b ₁	$\beta(\text{C}_2\text{-H}_4)(22)+\beta(\text{C}_3\text{-H}_5)(22)-\beta(\text{C}_8\text{-H}_9)(22)-\beta(\text{C}_7\text{-H}_6)(22)$
29	1260 (0.32,0.001) 0.75	1270 (5.11,0.001) 0.75	1285 (0,6.28) 0.75	-	1258 (w)	1295 (0,10.76) 0.75	a ₂	$\beta(\text{C}_8\text{-H}_9)(22)+\beta(\text{C}_7\text{-H}_6)(22)+\beta(\text{C}_3\text{-H}_5)(22)$
30	1556 (0.25,322.47) 0.23	1399 (0,734) 0.28	1573 (0.64,391) 0.18	-	1518 (vs) 0.14	1435 (0,260.51) 0.29	a ₁	$\nu(\text{C}_1\text{-C}_{10})(44)+\nu(\text{C}_2\text{-C}_3)(21)+\nu(\text{C}_7\text{-C}_8)(21)$
31	1579 (48.55,2.84) 0.75	1530 (80,0) 0.74	1592 (38.68,1.79) 0.75	1528 (m)	-	1534 (100.68,0) 0.67	b ₂	$\nu(\text{C}_7\text{-C}_8)(41)-\nu(\text{C}_2\text{-C}_3)(41)$
32	1590 (1.76,18.05) 0.34	1550 (0,550) 0.31	1616 (0.38,43.81) 0.73	-	1555 (m) 0.49	1553 (0,501.6) 0.27	a ₁	$\nu(\text{C}_1\text{-C}_{10})(38)-\nu(\text{C}_7\text{-C}_8)(20)-\nu(\text{C}_2\text{-C}_3)(20)+\alpha(\text{ring})(4)+\alpha(\text{ring})(4)$
33	3186 (0,252.16) 0.75	3196 (0,208.33) 0.75	3208 (0,218.95) 0.75	-	3072 (vw) 0.77	3215 (0.01,189) 0.75	a ₂	$\nu(\text{C}_2\text{-H}_4)(25)-\nu(\text{C}_3\text{-H}_5)(25)+\nu(\text{C}_8\text{-H}_9)(25)-\nu(\text{C}_7\text{-H}_6)(25)$
34	3186 (3.35,10.500) 0.75	3196 (23.34,0.02) 0.75	3208 (5.61,4.35) 0.75	3062 (m)	-	3215 (34.20,0.7) 0.75	b ₁	$\nu(\text{C}_8\text{-H}_9)(25)-\nu(\text{C}_7\text{-H}_6)(25)-\nu(\text{C}_2\text{-H}_4)(25)+\nu(\text{C}_3\text{-H}_5)(25)$
35	3208 (0.95,39.04) 0.75	3214 (45.62,0.9) 0.20	3228 (0.04,16.14) 0.75	-	-	3232 (70,0.09) 0.20	b ₂	$\nu(\text{C}_3\text{-H}_5)(25)+\nu(\text{C}_2\text{-H}_4)(25)-\nu(\text{C}_7\text{-H}_6)(25)-\nu(\text{C}_8\text{-H}_9)(25)$
36	3208 (0.01,693.302) 0.19	3214 (23.34,0.02) 0.75	3228 (0,593.35) 0.19	3080 (v w)	-	3231 (0.01,627) 0.19	a ₁	$\nu(\text{C}_7\text{-H}_6)(25)+\nu(\text{C}_8\text{-H}_9)(25)+\nu(\text{C}_3\text{-H}_5)(25)+\nu(\text{C}_2\text{-H}_4)(25)$

^δ : The first and second numbers within each bracket represent IR intensity and Raman activity, while the number before each bracket represent the corresponding calculated frequency (cm⁻¹), first and second words after each bracket represent corresponding species of the point group and depolarization ratios of the Raman band, respectively.

*ν = stretching, α = planar deformation of ring, τ = twisting about the central C=C bond, β = planar deformation of C=C/C-H, γ = non-planar deformation of the C=C/C-H, Φ = non-planar deformation of ring.

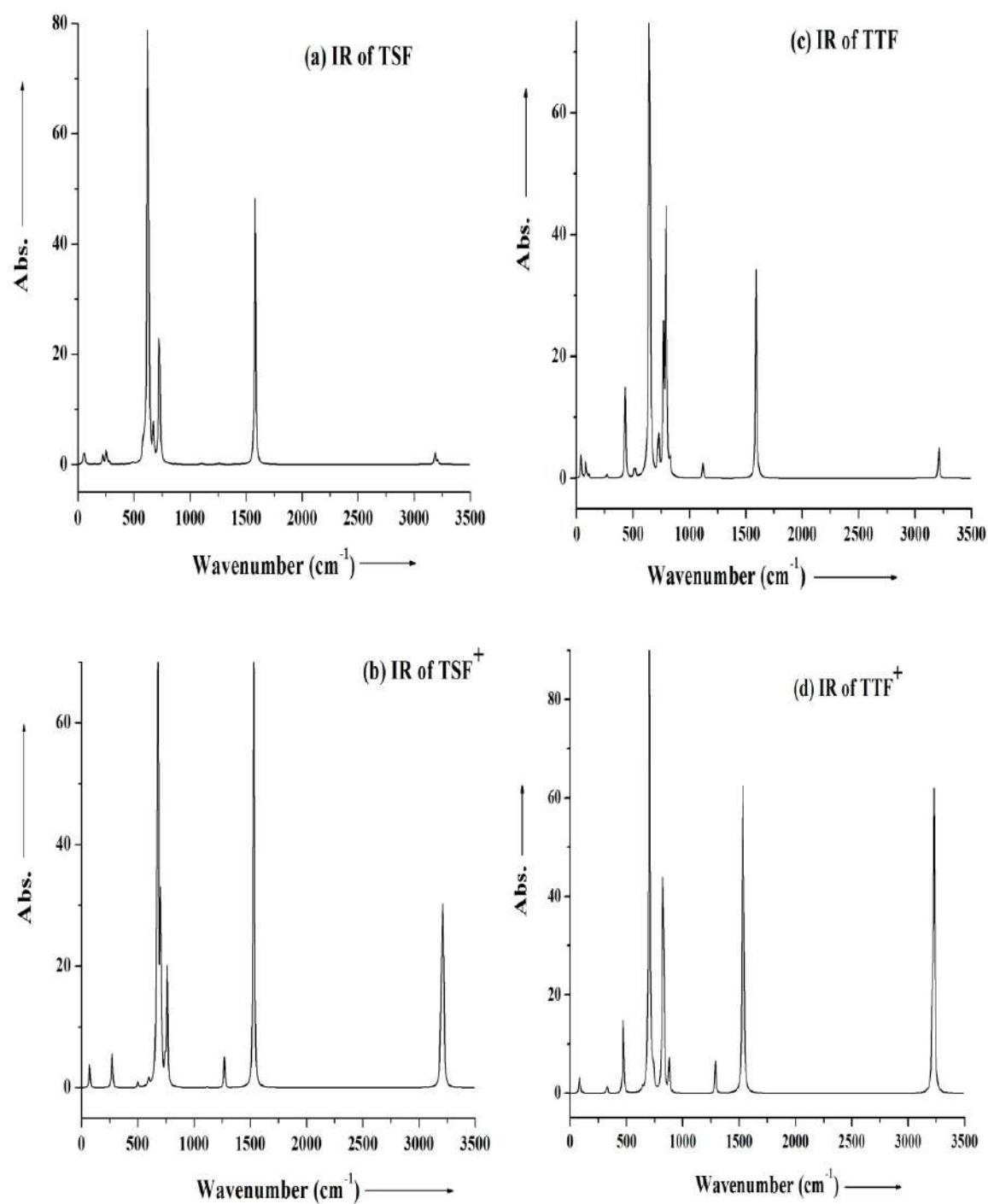


Fig 4. Calculated IR spectrum for (a) TSF, (b) TSF^+ , (c) TTF and (d) TTF^+

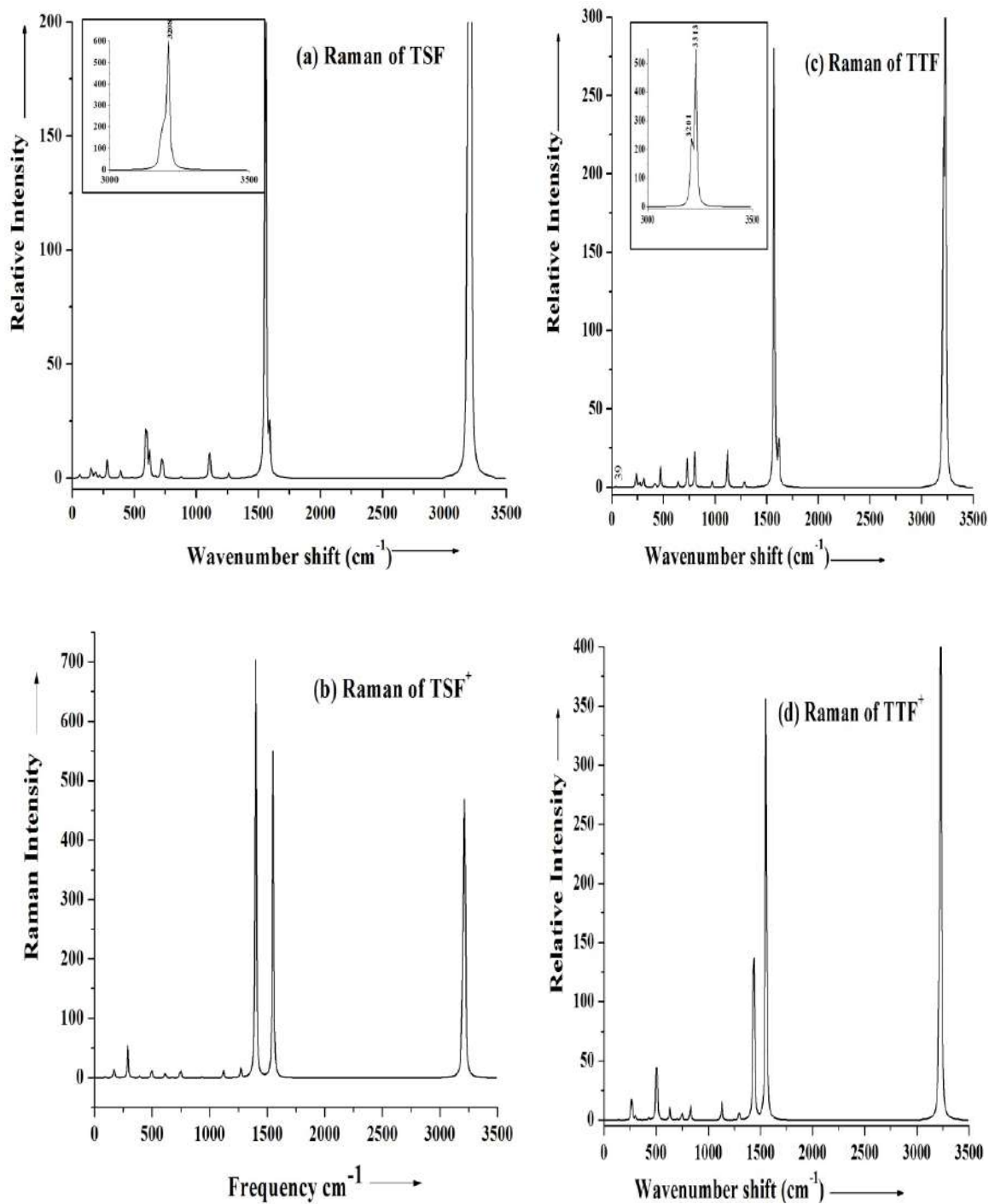


Fig 5. Calculated Raman spectrum for (a) TSF, (b) TSF⁺, (c) TTF and (d) TTF⁺

The neutral molecules belong to the C_{2v} point group of symmetry with non-planar structure. However, in going from the neutral molecule to its cation, the non-planar structure is deformed to the planar structure and point group of symmetry changes from C_{2v} to D_{2h} . All the 36 normal modes of the neutral molecules and their cations are distributed as;

$$\text{TSF: } 10a_1 + 9a_2 + 8b_1 + 9b_2$$

$$\text{TSF}^+: 7a_g + 2b_{1g} + 3b_{2g} + 6b_{3g} + 3a_u + 6b_{1u} + 6b_{2u} + 3b_{3u}$$

The atoms C_2, C_3, H_4, H_5 and H_6, C_7, C_8, H_9 are co-planar and similarly $C_1, C_{10}, \text{Se}/S_{11}, \text{Se}/S_{12}, \text{Se}/S_{13}, \text{Se}/S_{14}$ are co-planar in the neutral molecules. These two planes could be treated as local planes and all the normal modes have been discussed with respect to these planes [27].

3.4.1 C-H group modes

The C-H stretching vibrations are pure and highly localised modes. The present calculations place the four C-H stretching vibrations for the TSF molecule at the frequencies 3186, 3186, 3208, 3208 cm^{-1} under the symmetry species a_2, b_1, b_2, a_1 , respectively. The four corresponding $\nu(\text{C-H})$ frequencies for TTF are found at 3208, 3208, 3228, 3228 cm^{-1} . The frequencies of the $\nu(\text{C-H})$ modes are not affected much in going from neutral to their corresponding cations.

The frequencies of the four $\beta(\text{C-H})$ modes for the TSF and TTF are calculated to be 1105, 1105, 1259, 1260 cm^{-1} and 1120, 1121, 1283, 1285 cm^{-1} , respectively. All the $\beta(\text{C-H})$ bands are found with weak intensity in IR and as well in Raman spectra. In going from TSF to TTF, the two higher frequencies of $\beta(\text{C-H})$ modes are increased by 5 cm^{-1} , whereas the remaining two lower frequencies are increased by 15 cm^{-1} . The former frequencies are increased by ~ 14 and ~ 8 cm^{-1} and latter frequencies are increased by 10 and 10 cm^{-1} in going from TSF to TSF^+ and TTF to TTF^+ , respectively.

3.4.2 Ring modes

The TSF, TTF, TTF^+ molecules have two pentagon rings. The corresponding vibrations of the two rings couple together to give rise to the 18 normal modes of vibration as: $2 \times [5 \nu(\text{ring}), 2 \alpha(\text{ring})$ and $2 \Phi(\text{ring})]$ modes and also give rise to the 6 modes due to the central C=C bond.

The TSF and TTF molecules have two C=C bonds of rings and one central C=C bond, consequently, three $\nu(\text{C=C})$ modes (two under species a_1 and one under species b_2) are expected corresponding to these three C=C bonds. Out of these three $\nu(\text{C=C})$ modes, two modes under the species a_1 and b_2 are computed to be 1590 and 1579 cm^{-1} for TSF, and the remaining one mode under the species a_1 is computed as 1556 cm^{-1} for TSF.

The stretching frequencies corresponding to the remaining eight normal modes are equally distributed amongst the four species a_1, a_2, b_1 and b_2 of the C_{2v} point group i.e., each of these species contain two ring stretching modes arising due to the eight C-Se/S stretching motions. For the TSF molecule, the C-Se stretching modes are calculated to be 280, 581, 595, 672, 708, 724, 725, 879 cm^{-1} with the corresponding frequencies of the TTF molecule as 471, 726, 729, 772, 793, 799, 827 and 969 cm^{-1} , respectively. Out of the four ring deformation modes, the lower two modes arise due to the ring deformations in the plane of the Se/S atoms which are calculated to be 154 & 253 cm^{-1} and 237 & 434 cm^{-1} for TSF and TTF, while the higher two modes arise due to the ring deformation in the $\text{Se}/S_{13}\text{-C}_7\text{-C}_8\text{-Se}/S_{14}$ and $\text{Se}/S_{11}\text{-C}_2\text{-C}_3\text{-Se}/S_{12}$ planes which are calculated to be 483 & 487 and 613 & 623 cm^{-1} for TSF and TTF, respectively. There are four frequencies corresponding to four non-planar ring deformations due to the local planes which are calculated to be 388, 381, 60, 47 and 411, 416, 80, 39 cm^{-1} for the TSF and TTF molecules, respectively.

There are 6 modes associated with the two rings connecting with C=C bond as: a $\nu(\text{C=C})$, two $\beta(\text{C=C})$, two $\gamma(\text{C=C})$ and a $\tau(\text{C=C})$ modes. The frequency of the central (C=C) stretching mode of TSF is assigned at

the calculated frequency 1556 cm^{-1} . For the TTF molecule, the $\nu(\text{C}=\text{C})$ mode is assigned at the calculated frequency 1573 cm^{-1} and correlated to the observed medium Raman band 1518 cm^{-1} . The significant changes in vibrational frequencies of the C=C stretching modes accompanying the radicalization have been noticed. In going from TSF to TSF^+ and from TTF to TTF^+ , the frequency of the $\nu(\text{C}=\text{C})$ mode is increased by 150 and 138 cm^{-1} , respectively. According to the PEDs calculation, the two planar C=C bendings are found to be 76 and 185 cm^{-1} while these are found to have strongly increased magnitude in going from TSF to TTF. The two non-planar C=C bending modes are calculated to have the wavenumbers 222 and 472 cm^{-1} . The frequencies of $\gamma(\text{C}=\text{C})$ shift towards the higher frequency side in going from TSF to TTF and also in going from neutral to their corresponding cations. The $\tau(\text{C}=\text{C})$ mode is calculated to be 46 cm^{-1} with weak intensity for the TSF molecule. The magnitude of the frequency of the $\tau(\text{C}=\text{C})$ increases by 35 cm^{-1} in going from TSF to TTF, whereas this decreases by 23 and 38 cm^{-1} in going from TSF to TSF^+ and TTF to TTF^+ , respectively.

3.5 Vibronic Coupling

The Hamiltonian $H(r, R)$ of a molecule is given by,

$$H(r, R) = H_e(r, R) + T_n(R) \quad (1)$$

where $H_e(r, R)$ is an electronic Hamiltonian, $T_n(R)$ is the nuclear kinetic energy and r and R are sets of electronic and nuclear coordinates, respectively. The strength VCC ($\equiv V_i$) of the vibronic coupling (VC) with respect to the vibrational mode i is given by [41,42],

$$V_i = \left\langle \Psi \left| \left(\frac{\partial H_e(r, R)}{\partial Q_i} \right)_{R_0} \right| \Psi \right\rangle \quad (2)$$

where R_0 is the set of nuclear coordinates of the equilibrium geometry of the initial state, and Ψ is the electronic wavefunction corresponding to $H_e(r, R_0)$. Applying the Hellmann–Feynman theorem [43] V_i is written as,

$$V_i = \left(\frac{\partial E(r, R)}{\partial Q_i} \right)_{R_0} \quad (3)$$

$$= \sum_A \left(\frac{\partial E(r, R)}{\partial R_A} \right)_{R_0} \cdot \frac{u_A^i}{\sqrt{M_A}} \quad (4)$$

where $E(r, R)$ is the eigenvalue corresponding to the electronic Hamiltonian $H_e(r, R)$, R_A is the position of the A^{th} nucleus, u_A^i are the 3D components of the A^{th} nucleus, and M_A is the nuclear mass [44]. The Eq (3) is employed for calculation of the V_i .

The calculated V_i for the totally symmetric modes for transition from TSF to TSF^+ and from TTF to TTF^+ are listed in Table 4. The present results are indicated that the contribution to the vibronic coupling arises from all the modes; however, the $\nu(\text{ring})$ vibrational mode (motion of the C=C bonds of the ring dominate the motion of other bonds) has relatively larger V_i as compared to the other vibrational modes of both TSF and TTF. In going from a neutral molecule to its positively charged ion and vice versa the geometry is modified which involves relaxation energy. During the $\nu(\text{C}=\text{C})$ and $\nu(\text{ring})$ normal modes of vibration under the a_1 species the molecular geometry changes continuously between the two extreme configurations. During certain vibrational modes the geometries corresponding to the neutral molecule and its radical ion would lie between these two extreme configurations. The neutral molecule during such a vibrational mode may undergo electron transfer and yield its radical ion and vice versa without any excess requirement of activation/relaxation energy as and when its geometry becomes identical to the geometry of its radical ion.

Table 4. Calculated wavenumbers (cm^{-1}), vibronic coupling constants (VCCs) in 10^{-4} a.u. of all symmetric vibrational modes of $\text{TSF} \rightarrow \text{TSF}^+$ and $\text{TTF} \rightarrow \text{TTF}^+$

Mode No.	$\text{TSF} \rightarrow \text{TSF}^+$		$\text{TTF} \rightarrow \text{TTF}^+$		Modes
	wavenumbers	VCCs	wavenumbers	VCCs	
ν_1	47	0.08	39	0.04	$\Phi(\text{ring})$
ν_2	154	0.03	237	0.05	$\alpha(\text{ring})$
ν_3	222	0.52	267	0.08	$\gamma(\text{C}=\text{C})$
ν_4	280	0.19	472	0.01	$\nu(\text{ring})$
ν_5	595	0.17	644	0.15	$\gamma(\text{C}-\text{H})$
ν_6	624	0.01	729	0.02	$\nu(\text{ring})$
ν_7	1105	0.03	1121	0.06	$\beta(\text{C}-\text{H})$
ν_8	1556	1.34	1573	0.87	$\nu(\text{ring})$
ν_9	1590	0.52	1616	0.40	$\nu(\text{C}=\text{C})$
ν_{10}	3208	0.02	3228	0.04	$\nu(\text{C}-\text{H})$

4 Conclusions

From the present investigation it turned out that the neutral molecules possess non-planar structure with C_{2v} point group symmetry, whereas the cationic molecules possess planar structure with D_{2h} point group symmetry. The present calculations predicted that the energy gap of the TTF molecule is greater than the TSF molecule by 0.44 eV, Fig 3 and therefore, the TTF molecule is found to be kinetically more stable and chemically less reactive as compared to the TSF molecule. Furthermore, both the neutral molecules have tendency to lose electrons and hence, have same ionization potential but TSF would take electrons more easily as compared to the TTF molecule and therefore, it would have greater electron affinity.

The EMV or vibronic coupling and their roles in the occurrence of possible conductivity in the TSF and TTF molecules have been investigated. The vibrational modes $\nu(\text{ring})$ and $\nu(\text{C}=\text{C})$ under the species a_1 contribute to vibronic coupling. Large vibronic coupling constants of these modes show that removal of an electron from TSF and TTF is much easier during the excitation of above mentioned vibrational modes. The EMV interaction depends mainly on vibrational modes.

Acknowledgements

Poonam Rani is thankful to the Banaras Hindu University, Varanasi, India and UGC, New Delhi, India for providing financial support in the form of RF-SMS fellowship.

References

1. Bredás J L, Beljonne D, Coropceanu V, Cornil J, *Chem Rev*, 104(2004)2004.
2. Coropceanu V, Cornil J, da Silva Filho D A, Olivier Y, Silbey R, Bredás J L, *Chem Rev*, 107(2007)2007.
3. Ishii H, Sugiyama K, Ito E, Seki K, *Adv Mater*, 11(1999)605.
4. Cahen D, Kahn A, *Adv Mater*, 15(2003)271.
5. Adams D M, Brus L, Chidsey C E D, Creager S, Creutz C, Kagan C R, Kamat P V, Lieberman M, Lindsay S, Marcus R A, Metzger R M, Michel-Beyerle M E, Miller J R, Newton M D, Rolison D R, Sankey O, Schanze K S, Yardley J, Xu X, *J Phys Chem B*, 107(2003)6668.
6. Gershenson M E, Podzorov V, Morpurgo A F, *Rev Mod Phys*, 78(2006)973.
7. Moliton A, Hiorns R C, *Polym Int*, 53(2004)2004.

8. Cornil J, Lemaire V, Steel M C, Dupin H, Burquel A, Beljonne D, Brédas J L, in *Organic Photovoltaics: Mechanisms, Materials, and Devices*, (eds) Sun S, Sariciftci N S, (Dekker, New York), 2005.
9. Tretiak S, Mukamel S, *Chem Rev*, 102(2002)3171.
10. Scholes G D, Rumbles G, *Nat Mater*, 5(2006)683.
11. Bittner E R, Ramon J G S, *Springer Ser Chem Phys*, 83(2007)57.
12. Scholes G D, *Annu Rev Phys Chem*, 54(2003)57.
13. Schwartz B J, *Annu Rev Phys Chem*, 54(2003)41.
14. Hennebicq E, Pourtois G, Scholes G D, Herz L M, Russell D M, Silva C, Setayesh S, Grimsdale A, Müllen K, Brédas J-L, Beljonne D, *J Am Chem Soc*, 127(2005)4744.
15. Hoebein F J M, Jonkheijm P, Meijer E W, Schenning A P H J, *Chem Rev*, 105(2005)1491.
16. Cornil J, Beljonne D, Calbert J P, Brédas J L, *Adv Mater*, 13(2001)1053.
17. Milián-Medina B, Van Vooren A, Brocorens P, Gierschner J, Shkunov M, Heeney M, McCulloch I, Lazzaroni R, Cornil J, *Chem Mater*, 19(2007)4949.
18. Scheblykin I G, Yartsev A, Pullerits T, Gulbinas V, Sundström V, *J Phys Chem*, B111(2007)6303.
19. Friend R H, Gymer R W, Holmes A B, Burroughes J H, Marks R N, Taliani C, Bradley D D C, dos Santos D A, Brédas J L, Lögdlund M, Salaneck W R, *Nature (London)*, 397(1999)121.
20. Gierschner J, Cornil J, Egelhaaf H-J, *Adv Mater*, 19(2007)173.
21. Sancho-García J C, Pérez-Jiménez A J, *J Chem Phys*, 129(2008)024103.
22. Brédas J L, Street G B, *Acc Chem Res*, 18(1985)309.
23. Devos A, Lannoo M, *Phys Rev B*, 58(1998)8236.
24. Kato T, Yamabe T, *J Chem Phys*, 115(2001)8592.
25. Bässler H, *Phys Status Solidi*, B175(1993)15.
26. Martorell B, Fraxedas J, Clotet A, *Surface Science*, 605(2011)187.
27. Rani P, Yadav R A, *Spectrochim Acta*, A99(2012)303.
28. Frisch M J, Trucks G W, Schlegel H B, Scuseria G E, Robb M A, Cheeseman J R, Montgomery J A, (Jr), Vreven T, Kudin K N, Burant J C, Millam J M, Iyengar S S, Tomasi J, V. Barone V, Mennucci B, Cossi M, Scalmani G, Rega N, Petersson G A, Nakatsuji H, Hada M, Ehara M, Toyota K, Fukuda R, Hasegawa J, Ishida M, Nakajima T, Honda Y, Kitao O, Nakai H, Klene M, Li X, Knox J E, Hratchian H P, Cross J B, Bakken V, Adamo C, Jaramillo J, Gomperts R, Stratmann R E, Yazyev O, Austin A, Cammi J R, Pomelli C, Ochterski J W, Ayala P Y, Morokuma K, Voth G A, Salvador P, Dannenberg J J, Zakrzewski V G, Dapprich S, Daniels A D, Strain M C, Farkas O, Malick D K, Rabuck A D, Raghavachari K, Foresman J B, Ortiz J V, Cui Q, Baboul A G, Clifford S, Cioslowski J, Stefanov B B, Liu G, Liashenko A, Piskorz P, Komaromi I, Martin R L, Fox D J, Keith T, Al-Laham M A, Peng C Y, Nanayakkara A, Challacombe M, Gill P M W, Johnson B, Chen W, Wong M W, Gonzalez C, Pople J A, Gaussian, Inc., Wallingford CT, 2004.
29. Frisch A, Nielsen A B, Holder A J, GaussView user manual, Gaussian, Inc., Pittsburgh, PA, 2000.
30. Martin J M L, Alsenoy V, Alsenoy C V, GAR2PED University of Antwerp, 1995.
31. Ferreira M M C, Sato E, *J Phys Chem*, 96(1992)8844.
32. Pedregosa J C, Alzuet G, Borrás J, Fustero S, Granda S G, Diaz M R, *Acta Crystallogr C*, 49(1993)630.
33. Nakayama A, Hagiwara K, Hashimoto S, Shimoda S, *Quant Struct Act Relat*, 12(1993)251.
34. Fukui K, *Theory of Orientation and Stereoselection*, (Springer Verlag, New York), 1975.
35. Raghunath P, Reddy M A, Gauri C, Bhanuprakash K, Rao V J, *J Phys Chem A*, 110(2006)1152.
36. Foresman J B, Frisch A E, *Exploring Chemistry with Electronic Structure Methods*, 2nd edn., Gaussian, Pittsburgh, PA, 1996.
37. Lewars E, *Computational Chemistry — Introduction to the Theory and Applications of Molecular and Quantum Mechanics*, (Kluwer Academic Publishers, Norwell, MA), 2003.
38. Manolopoulos D F, May J C, Down S E, *Chem Phys Lett*, 181(1991)1991.
39. Chang R, *Chemistry*, 7th edn, (McGraw-Hill, New York), 2001.

40. Koopmans T, *Physica*, 1(1933)104.
41. Bersuker I B, *The Jahn–Teller Effect*, (Cambridge University Press, Cambridge), 2005.
42. Sato T, Tokunaga K, Iwahara N, Shizu, Tanaka K H, *The Jahn–Teller Effect: Fundamentals and Implications for Physics and Chemistry*, (Springer-Verlag, Berlin), 2009.
43. Feynman R P, *Phys Rev*, 56(1939)340.
44. Iwahara N, Sato T, Tanaka K, Chibotaru L F, *Phys Rev B*, 82(2010)245409.

[Received :20.1.2015; revised recd: 28.4.2015; accepted : 30.5.2015]